ISSN 1070-3284, Russian Journal of Coordination Chemistry, 2020, Vol. 46, No. 9, pp. 622–630. © Pleiades Publishing, Ltd., 2020.
Russian Text © The Author(s), 2020, published in Koordinatsionnaya Khimiya, 2020, Vol. 46, No. 9, pp. 545–553.

New Ternary Bismuthides NaZnBi and NaCdBi: Synthesis and Crystal Structures

A. I. Shilov[a, b, *], K. S. Pervakov[b], V. A. Tafeenko[a], and I. V. Morozov[a, **]

[a] *Moscow State University, Moscow, 119991 Russia*

[b] *Ginzburg Center for High-Temperature Superconductivity and Quantum Materials, Lebedev Physical Institute, Russian Academy of Sciences, Moscow, 119991 Russia*

**e-mail: tanknbp@live.com*

***e-mail: morozov@inorg.chem.msu.ru*

Received December 10, 2019; revised February 20, 2020; accepted March 25, 2020

Abstract—Single crystals of new ternary bismuthides NaZnBi (**I**) and NaCdBi (**II**) are obtained by the self-flux technique. Its crystal structures are studied by single-crystal X-ray structure analysis (CIF file CCDC nos. 1956988 (**I**) and 1956989 (**II**)). The synthesized compounds form isostructural series with lighter pnictide analogs. Similarly to NaZnPn (*Pn* = P, As, Sb), compound **I** crystallizes in the structural type PbFCl, space group $P4/nmm$, $a = 4.5114(5)$, $c = 7.5970(10)$ Å, whereas compound **II**, as NaCdPn (*Pn* = As, Sb), can be assigned to the structural type MgSrSi, space group *Pnma*, $a = 8.0812(5)$, $b = 4.8026(3)$, $c = 8.7320(7)$ Å. The crystal structure of compound **I** consists of antifluorite-like layers [ZnBi] separated by a layer of sodium atoms, whereas hexagonal corrugated [CdBi] layers, which are tightened between each other by Cd–Bi bonds with the formation of channels in which sodium atoms are localized, can be distinguished in the structure of compound **II**. The crystal structures of the synthesized bismuthides are compared both between each other and with lighter representatives of the isostructural series.

Keywords: ternary bismuthides, NaZnBi, NaCdBi, single crystal growth, X-ray structure analysis, crystal structure

DOI: 10.1134/S1070328420090043

INTRODUCTION

Compounds of the general composition ATPn (A is alkaline metal, T is *d* element, and Pn is pnictide) manifest a large variety of structures and properties due to the formation of diverse coordination polyhedra by the component atoms and their mutual arrangement. Among them there are insulators, semiconductors, compounds with metallic behavior, and superconductors. They can exhibit thermoelectric and diverse magnetic properties. The most known materials are layered iron-containing superconductors AFePn (Pn = P, As; A = Li, Na) that crystallize in the structural type PbClF (space group $P4/nmm$) [1], a wide family of manganese derivatives AMnPn (A is alkaline metal, Cu; Pn = P, As, Sb, Bi) manifesting the properties of semiconductor antiferromagnetics [2–4], and half-Heusler compounds characterized by the antifluorite-like structure (space groups $Fm\bar{3}m$ and $F\bar{4}3m$) and manifesting various physical properties, including those caused by the non-trivial Fermi surface topology [5]. The family of layered pnictides ATPn is of special interest. They contain hexagonal layers [TPn] built of alternating T and Pn atoms and A atoms arranged between these layers (family ZrBeSi, space group $P6_3/mmc$), and the layers can be tightened by interlayer T–Pn bonds to form framework centro- or noncentrosymmetric structures (families MgSrSi and LiGaGe, space groups *Pnma* and $P6_3mc$, respectively) manifesting antisegneto- and segnetoelectric properties [2, 6].

The thermodynamic stability of a series of ATPn compounds obeying the Zintl formalism, according to which the sum of valent electrons per formula unit is 8 or 18, was predicted on the basis of the already known structural data and theoretical calculations in the recently published works [7]. It was predicted that these compounds exhibited nontrivial functional properties [5]. Among these compounds, we were interested in bismuthides NaTBi, where T is Zn and Cd. Although the lighter pnictides of similar composition NaTPn (Pn = As, Sb) were synthesized earlier [8–10], bismuth derivatives remained unknown. Meanwhile, the transition to heavy pnictides leads to a regular change in the properties and can induce the appearance of new peculiarities, in particular, properties caused by the non-trivial Fermi surface topology. In addition, these compounds can be efficient mild

reducing agents for the synthesis of bismuth clusters using nonaqueous solvents.

In this work, we synthesized for the first time single crystals of NaZnBi (**I**) and NaCdBi (**II**) and determined their crystal structures. In spite of the same stoichiometry and similarity of the coordination polyhedra of the component atoms Na, Zn/Cd, and Bi, these compounds are of various structural types. A comparison of the crystal structures of the synthesized compounds with the lighter representatives of the isostructural series makes it possible to reveal certain factors affecting the accomplishment of this or another structural type in ternary pnictides ATPn (A is alkaline metal; T = Zn, Cd).

EXPERIMENTAL

Synthesis. All procedures on the preparation of the initial reaction mixtures, separation of the synthesized compounds from by-products, and preparation of the synthesized samples for further studies were carried out in a dry argon box with the water content not higher than 0.1 ppm and oxygen content at most 0.5 ppm. The metallic reagents Na (99.95%), Zn (99.9%) or Cd (99.9%), and Bi (99.95%) in the molar ratio Na : (Zn/Cd) : Bi = 1 : 1 : 6 were placed in an annealed alumina crucible, the upper part of which was closed with quartz wool for the further separation of the flux by centrifugation, after which the crucible was placed in a quartz ampule, which was evacuated, filled with dry argon to a residual pressure of 0.1 atm, and sealed. Then the ampule with the crucible inside was placed in a muffle furnace and heated up to 873 K within 24 h, kept at this temperature for 48 h for the homogenization of the melt, and cooled down to 573 K with a rate of 2 K/h. Excess bismuth was removed by high-temperature centrifugation.

After the end of the reaction and centrifugation of the melt in the case of the Na–Zn–Bi system, blocks of layered crystals of NaZnBi (**I**) were taken from the crucible. The blocks with metallic luster of regular rectangular shape up to 1 cm in size were easily separated from one another using a scalpel (Fig. 1a). The obtained crystals were very unstable in air and decomposed within several minutes and, hence, all operations were carried out in a dry box in an argon atmosphere.

The X-ray diffraction analysis (XRD) of the polycrystalline sample obtained by grinding of the selected single crystals in a mortar was carried out on a Rigaku MiniFlex 600 diffractometer (graphite monochromator, CuK_α radiation). The sample was placed in a airtight holder inside the dry box to protect from contact with open air. The obtained XRD pattern indicated that the sample is single-phase and well indexed in the space group *P*4/*nmm* with the crystal cell parameters close to those of NaMnBi [3].

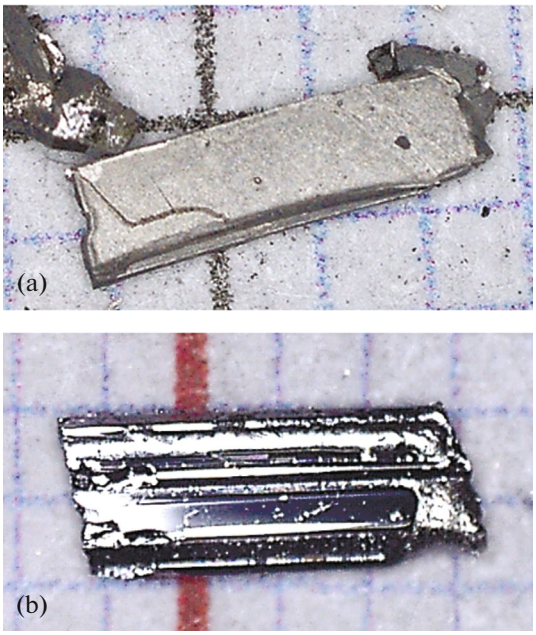

Fig. 1. Crystals of compounds (a) **I** and (b) **II**.

In the case of the Na–Cd–Bi system, gray crystals of NaCdBi (**II**) of irregular shape with the sizes up to 2 × 2 × 5 mm were separated by centrifugation (Fig. 1b). Unlike compound **I**, complex **II** was more stable and demonstrated appreciable indications of degradation only after several hours of exposure in air, which is explained, as became clear further, by different structures of the compounds. The XRD of the grinded single crystals confirmed that the new, earlier unknown substance with the assumed composition of compound **II** was obtained. The composition and structure of the obtained single crystals were finally determined on the basis of the X-ray structure analysis data.

X-ray structure analysis. Single crystals of compounds **I** and **II** with linear sizes of ~0.1 mm were placed (under a microscope) in glass capillaries wetted with anhydrous paraffin oil, after which the capillaries were sealed. The set of X-ray structure data was collected on a STOE single-crystal diffractometer equipped with a Pilatus 100K detector, a graphite monochromator, and a collimator with a capillary diameter of 0.5 mm using MoK_α radiation. The structures were solved using the SHELXL2014 and SHELXT program packages and refined by least squares using the SHELXL2014 program package [11, 12]. The anisotropic model was applied after several refinement cycles in the isotropic approximation for the thermal vibration parameters of atoms. As a result of the refinement, the R_{int}-factors were 0.0516 and 0.043 for compounds **I** and **II**, respectively. The crystallographic data and structure refinement parameters of **I** and **II** are presented in Table 1. The characteristic interatomic distances are given in Table 2.

Table 1. Crystallographic data and structure refinement parameters for **I** and **II**

Parameter	**I**	**II**
Crystal system	Tetragonal	Orthorhombic
Space group	*P*4/*nmm*	*Pnma*
T, K	294	294
a, Å	4.5114(5)	8.0812(5)
b, Å	4.5114(5)	4.8026(3)
c, Å	7.597(1)	8.7320(7)
V, Å^3	154.62(4)	338.90(4)
Z	2	4
μ, mm^{-1}	64.39	57.95
Crystal size, mm	0.08 × 0.04 × 0.03	0.1 × 0.06 × 0.04
Information on data collection		
Absorption correction	Difabs	Multi scan
T_{min}, T_{max}		0.737, 0.823
Number of measured, independent, and observed ($I > 2\sigma(I)$) reflections	177, 177, 164	505, 505, 432
R_{int}	0.0516	0.043
$(\sin\theta/\lambda)_{max}$, Å^{-1}	0.728	0.683
R ($F^2 > 2\sigma(F^2)$), wR (F^2), S	0.052, 0.138, 1.15	0.038, 0.102, 1.07
Number of refined parameters	10	19
$\Delta\rho_{max}$, $\Delta\rho_{min}$, e Å^{-3}	2.70, −2.73	1.75, −2.04

Table 2. Characteristic interatomic distances in **I** and **II**

I		**II**	
Bond	*d*, Å	Bond	*d*, Å
Zn(1)−Bi(1)	4 × 2.8383(7)	Cd(1)−Bi(1)	2 × 2.9571(16)
			2.9699(17)
			3.0391(17)
Na(1)−Bi(1)	3.280(17)	Na(1)−Bi(1)	3.256(9)
	4 × 3.307(4)		2 × 3.400(6)
			2 × 3.468(6)

The coordinates of atoms and other parameters for the structures of compounds **I** and **II** were deposited with the Cambridge Crystallographic Data Centre (CIF files CCDC nos. 1956988 (**I**) and 1956989 (**II**); deposit@ccdc.cam.ac.uk or http://www.ccdc.cam.ac.uk/data_request/cif).

RESULTS AND DISCUSSION

Compound **I** crystallizes in the structural type PbFCl [7] (space group *P*4/*nmm*) and consists of anti-fluorite-like layers [ZnBi] with interlayers of Na atoms. In the layers, the Zn atoms form a planar network and the Bi atoms are arranged in staggered rows above and under the centers of the [Zn_4] squares due to which each Zn atom has a tetrahedral environment of four Bi atoms (Fig. 2). The tetrahedral polyhedron [$ZnBi_4$] is somewhat extended along the inversion C_{4i} axis passing parallel to the *c* axis through two opposite edges of the tetrahedron. This is indicated by the values of two BiZnBi angles (105.26(4)°) leaned on these edges. The extension of the tetrahedron somewhat increases in the pnictide series NaZnPn with an increase in the size of Pn (Table 3). The Na atoms are arranged between the [ZnBi] layers to form the coordination polyhedron [$NaBi_5$] as a square pyramid,

whose base is formed by four Bi atoms from one layer, and the fifth bismuth atom from the adjacent layer occupies the axial vertex (Fig. 2). The C_4 axis passes parallel to the *c* axis through the vertex of the pyramid and the middle of the base. The geometric parameters of the pyramid are presented in Tables 2 and 3 and show that the distances from the Na atom to the basal Bi atoms lying in the pyramid base (l_b) only insignificantly exceed the distance to the Bi atom in the axial vertex (ratio $l_a/l_b = 0.99$). The bismuth atom is situated inside the monocapped square antiprism [$BiZn_4Na_5$] (Fig. 3a). The bottom base of the antiprism is formed by four Zn atoms, and the upper base and capped vertex are formed by the Na atoms. The [$BiZn_4Na_5$] polyhedron is oriented along the *c* axis in such a way that the axis of rotation C_4 passes through the middle of the [Zn_4] square and capped vertex. It should be mentioned that NaZnBi is isostructural to the manganese derivative NaMnBi [3], but the unit cell size and interatomic distances of the latter are somewhat higher because of the larger size of the Mn atom compared to Zn [14, 15].

The replacement of the zinc atom by cadmium substantially changes the crystal structure: compound **II**, as well as its lighter analogs NaCdPn (Pn = As, Sb), crystallizes in the structural type MgSrSi (orthorhombic crystal system *Pnma*). The corrugated hexagonal layers in which each Bi atom is linked with three Cd atoms and vice versa can be distinguished in the structure of compound **II** (Fig. 4). The layers are parallel to the plane (*bc*) and oriented in such a way that series of translationally bound Cd (or Bi) atoms are formed along the *b* direction at the same height *x*. The cadmium atoms, along with three Cd–Bi bonds in the layer, form the fourth bond with the bismuth atom from the higher- or lower-lying layer thus completing the coordination to a distorted tetrahedron. In the [$CdBi_4$] tetrahedron, one of the Bi···Bi edges and

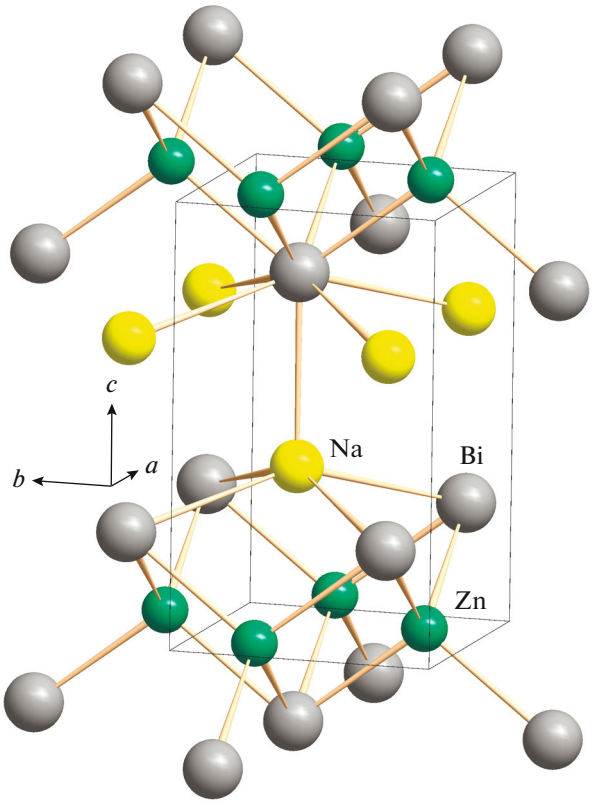

Fig. 2. Crystal structure of compound **I**.

the Cd atom lie in the symmetry plane. The average Cd–Bi bond length (2.98 Å) exceeds the Zn–Bi bond length in compound **I** (2.84 Å) by 0.14 Å, which correlates with an increase in the ionic radius by 0.18 Å [14, 15] on going from Zn^{2+} to Cd^{2+}.

Channels directed along the *b* axis are formed due to the Cd–Bi bonds between the adjacent hexagonal [CdBi] layers. The sodium atoms are located in these

Table 3. Comparison of the unit cell parameters and characteristic bond lengths (Å) and bond angles (deg) in the series of isostructural pnictides NaZnPn, where Pn is P, As, Sb, and Bi (structural type PbClF, space group *P*4/*nmm*)

Pn	*a* *c*	*c*/*a*	$R(Pn^{3-})$*	Zn–Pn**	2 × PnZnPn	Zn–Zn	1 × Na–Pn (l_a)	4 × Na–Pn (l_b)	l_a/l_b	References
P	4.012 6.801	1.695	1.71(4)	2.473 (2.45)	108.41	2.837	2.913	3.006	0.97	[13]
As	4.122 6.995	1.697	1.81(2)	2.537 (2.55)	108.65	2.914	3.003	3.092	0.97	[10]
Sb	4.365 7.363	1.687	1.974(8)	2.722 (2.714)	106.59	3.087	3.181	3.223	0.99	[9]
Bi	4.511 7.597	1.684	2.08(2)	2.8383 (2.82)	105.261	3.190	3.280	3.307	0.99	This work

* The effective radii of pnictide Pn^{3-} in the structures NaTPn (T = Zn, Mn, Cd) were estimated using the structural data from the Inorganic Crystal Structure Database (ICSD) and effective ionic radii of the cations T^{2+} (coordination number 4), which are 0.74, 0.80, and 0.92 Å for B = Zn, Mn, and Cd, respectively [14, 15]. ** The Zn–Pn bond lengths calculated as the sum of $R(Pn^{3-})$ and $R(Zn^{2+})$ are given in parentheses.

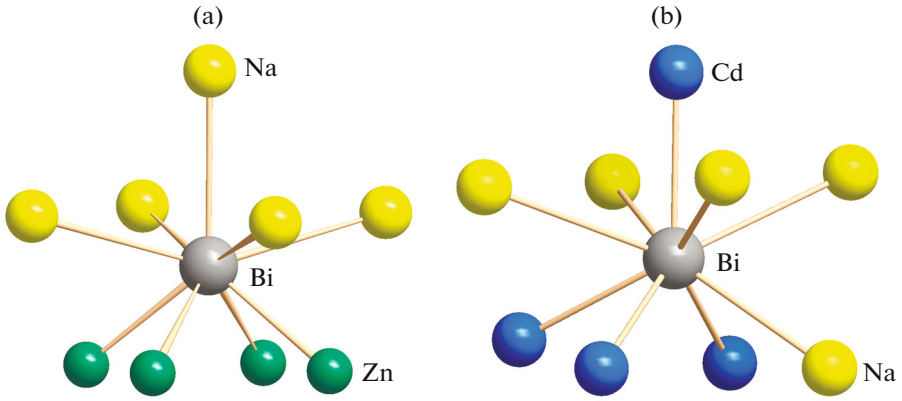

Fig. 3. Structures of the coordination polyhedra of bismuth in compounds (a) **I** and (b) **II**.

channels and coordinate five bismuth atoms to form a distorted tetragonal pyramidal polyhedron [$NaBi_5$]. The base of the pyramid is a rectangle, one side of which belongs to one [CdBi] layer and the second side and axial vertex belong to another layer (Fig. 4c). A comparison of the data in Tables 3 and 4 shows that the lengths of the Na–Bi bonds to the basal Bi atoms increased appreciably (by 4%) in the pyramid of the structure **II** compared to the similar square pyramid [$NaBi_5$] in the structure **I**, whereas the Na–Bi distance to the axial vertex somewhat decreased (by 0.8%). These changes affected the l_a/l_b parameter, which is 0.94–0.95 for the NaCdPn structures, unlike 0.97–0.99 for the NaZnPn structures (Tables 3, 4).

The polyhedra of bismuth [$BiNa_5Cd_4$] also noticeably change in two considered structures. The polyhedron in the structure of compound **II** is less symmetric and also can be considered as a monocapped square antiprism. However, unlike the structure of compound **I**, the bottom base contains three Cd atoms and one Na atom; the upper base includes four Na atoms, and cadmium is located in the capped vertex (Fig. 2b).

It should be mentioned that the Bi–T (T = Zn, Cd) and Bi–Na bond lengths in compounds **I** and **II** are typical of similar compounds. For example, in Na_3Bi the Bi–Na bond lengths range from 3.15 to 3.53 Å [16], and the range of Bi–Cd in $Ba_2Cd_3Bi_4$ is 2.93–3.38 Å [17]. It seems interesting to compare the change in the unit cell parameters, characteristic bond lengths, and bond angles in the pnictide series NaTPn (T = Zn, Mn, Cd; Pn = P, As, Sb, Bi). For convenience of comparison, we estimated the effective radii of the Pn^{3-} anions. In these compounds, $R_{eff}(Pn^{3-}$, coordination number 9) were determined as the T–Pn bond lengths minus effective ionic radii $R_{eff}(T^{2+}$, coordination number 4) [13, 14], and the obtained values were averaged (Table 3).

The changes in the unit cell parameters in the NaTPn series (T = Zn, Cd) at various $R_{eff}(Pn^{3-})$ are presented in Fig. 5. It can be seen that the unit cell sizes of ternary pnictides NaTPn increase linearly with an increase in the pnictogen size (Figs. 5a, 5b), and for T = Zn the *c*/*a* ratio remains nearly unchanged

Table 4. Comparison of the unit cell parameters and characteristic bond lengths (Å) in the series of isostructural pnictides NaCdPn, where Pn is As, Sb, and Bi (structural type MgSrSi, space group *Pnma*)

Pn	*a* *b* *c*	*c*/*a*	*b*/*a*	2 × Cd–Pn Cd–Pn Cd–Pn	1 × Na–Pn*	2 × Na–Pn 2 × Na–Pn	l_a/l_b average	References
As	7.576 4.471 8.044	1.062	0.590	2.7327 2.7253 2.8253	3.022 (2.95)	3.204 3.236	0.94	[10]
Sb	7.940 4.704 8.420	1.059	0.592	2.8639 2.8695 2.9765	3.167 (3.11)	3.336 3.438	0.94	[10]
Bi	8.081 4.803 8.732	1.081	0.594	2.9571 2.9699 3.0391	3.256 (3.22)	3.400 3.468	0.95	This work

* The Na–Pn bond lengths calculated as the sum of $R(Na^+)$ and $R(Pn^{3-})$ are given in parentheses.

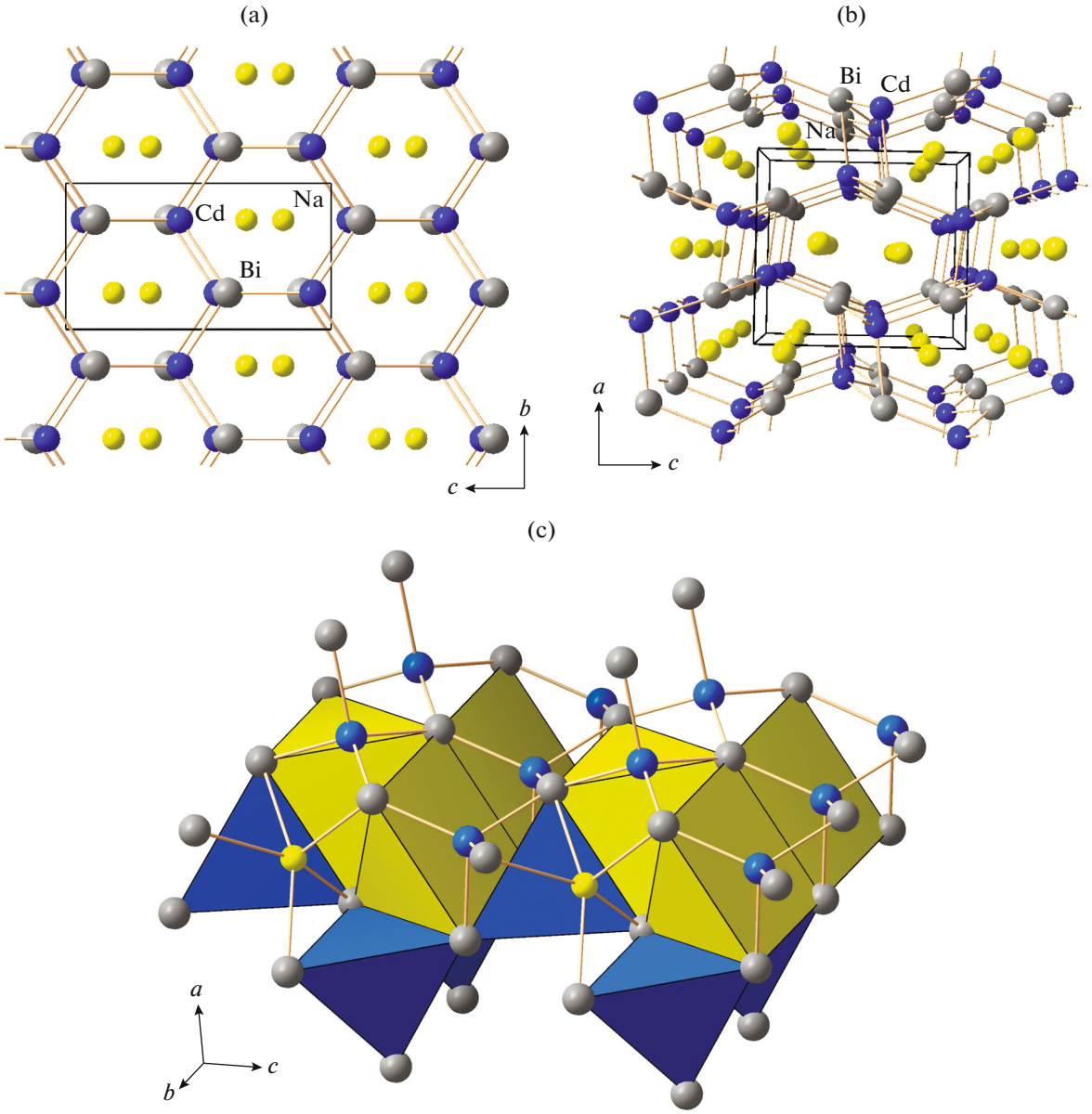

Fig. 4. Crystal structure of compound **II**: (a) projection along the *a* axis, (b) projection along the *b* axis, and (c) arrangement of Na atoms between the hexagonal [CdBi] layers. The coordination polyhedra are given for some Cd (blue) and Na (yellow) atoms.

(Table 3). The Zn···Zn distance ($|Zn–Zn| = a/\sqrt{2}$) regularly increases from 2.85 to 3.3 Å with an increase in the pnictogen size, which can affect the manifested physical properties. In the series of the isostructural manganese derivatives NaMnPn, the elongation of the Mn···Mn distance results in a regular decrease in the magnetic interaction, which is expressed as an increase in the effective magnetic moment [18–20].

A comparison of the structures of compounds **I** and **II** shows that in both modifications (*P*4/*nmm* and *Pnma*) the Na, Zn/Cd, and Bi atoms form similar coordination polyhedra, which possibly indicates a similar thermodynamic stability of both modifications. Nevertheless, a question arises: what induces the change of one structural modification by another? The answer is related, most likely, to a decrease in the stability of the [$NaBi_5$] polyhedron. In fact, a comparison of the tetragonal pyramidal coordination polyhedra [$NaBi_5$] in two studied structures shows that the bonds of sodium with the basal Bi atoms are noticeably weakened in the [$NaBi_5$] pyramid in the structure of compound **II**. The length of these bonds substantially exceeds the Na–Bi bond length calculated as the sum of effective ionic radii, whereas the Na–Bi distance to the axial vertex and the Na–Bi bond lengths in the structure of compound **I** quite correspond to the calculation (Table 4). The elongation of the Na–Bi

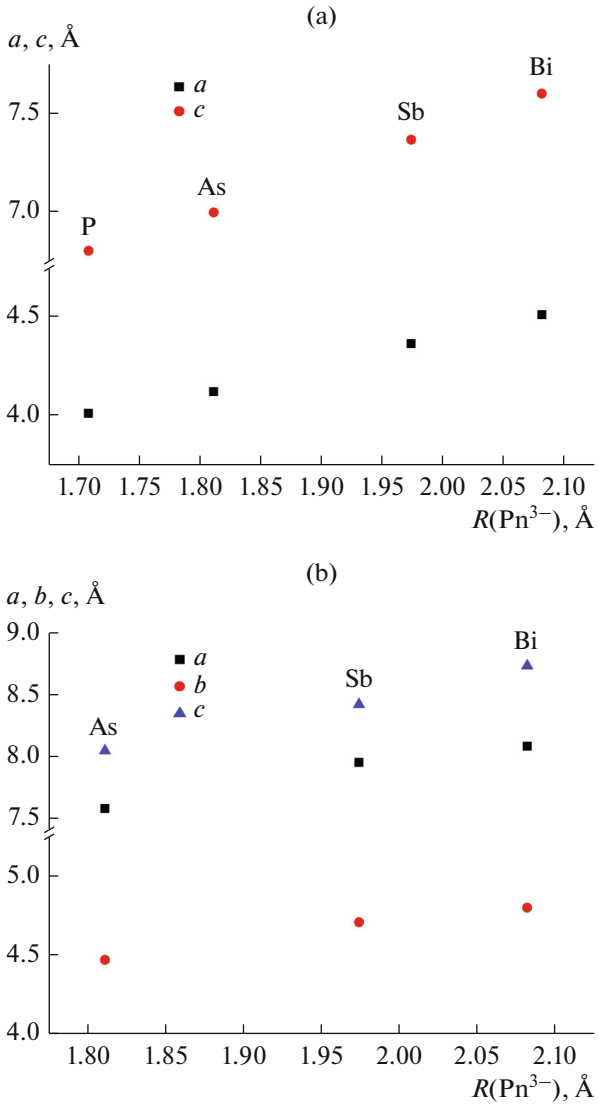

Fig. 5. Dependences of the unit cell parameters on the pnictide size in the series (a) NaZnPn and (b) NaCdPn.

bonds is associated with the fact that the sizes of the rectangular base [Bi_4] increase on going from Zn to Cd, since its sides are simultaneously the edges of four tetrahedra [$CdBi_4$]. An increase in the size of the T^{2+} cation on going from Zn to Cd results in the elongation of the Bi···Bi edge. In turn, the Na–Bi_b bond length should exceed half a diagonal of the pyramid base for the stability of the square pyramid. As a result, the sodium atom is hardly retained inside the tetragonal pyramid due to a considerable increase in the $NaBi_b$ bond lengths. Thus, a probable reason for the change in the structural type is that in the layered structures of the PbClF type the sodium cations provide layer binding along the *c* axis due to fairly strong Na–Pn bonds. The stability of the tetragonal pyramid [$NaPn_5$] decreases upon the replacement of Zn by Cd, and (although sodium forms a similar polyhedron) the framework structure takes place in which the Cd–Bi bonds play a serious role in the formation of 3D bonding.

Interestingly, the structural type PbClF (*P*4/*nmm*) is observed for all manganese derivatives AMnPn regardless of the choice of alkaline metal A (A = Na, K, Rb, Cs) and pnictide. It is most likely that the enhanced stability of this structural type is related, in the case of Mn, to an additional stabilization due to the magnetic interaction: in the layered structure of this type, the *d*-element atoms form planar square networks in which the interaction between the metal atoms with the long-range magnetic order is observed [21]. For other 3*d* elements, the formation of the ATPn derivatives in the structural type PbClF is characteristic only of light alkaline metals and pnictides of the beginning of the series: P and As. The reason for the fact that the structure of the PbClF type is not characteristic of large alkaline metal cations is that these cations tend to form polyhedra with higher coordination numbers. For example, in the case of T = Fe, compounds AFePn (Pn = P, As) are known for A = Li and Na only. As the alkaline metal size increases, compounds AFe_2Pn_2 (A = K, Rb, Cs) also containing fluorite-like layers [FePn] are observed, but the alkaline metal cations form the coordination polyhedron as a rectangular parallelepiped (coordination number 8). In the case of the zinc and cadmium derivatives, there is no additional stabilization of the structures due to the magnetic interactions and, thus, the dimensional factor is more important. The available published data supplemented by our results show that the ratio of sizes of the alkaline metal cation and *d* element are decisive, whereas the pnictogen sizes play the secondary role. Therefore, it is indicative that the KCdPn and NaZnPn series for which $R_{eff}(A^+)/R_{eff}(T^{2+})$ is 1.65 and 1.54, respectively, are isostructural (Table 5). The data presented in Table 5 show that with a decrease in the ratio of effective ionic radii $R_{eff}(A^+)/R_{eff}(T^{2+})$ for compounds ATPn the structural types are accomplished consequently in which the coordination numbers of cations of alkaline metal A decrease and, correspondingly, their crystal-chemical role changes. The structures with the high ratio $R_{eff}(A^+)/R_{eff}(T^{2+})$ are layered and contain hexagonal (KZnPn) or antifluorite-like (NaZnPn and KCdPn) [TPn] layers separated by interlayers of alkaline metal atoms. The structures become framework (NaCdPn, LiTPn) with a decrease in the $R_{eff}(A^+)/R_{eff}(T^{2+})$ ratio. The LiTPn structures can be considered as three-dimensional frameworks consisting of tetrahedra [$TPn_{4/4}$] with common vertices packed according to the wurtzite (space group $P6_3mc$) or sphalerite (space group $F\bar{4}3m$) motif [22, 23], and the Li atoms are located in the octahedral or tetrahedral cavities, respectively, of the anionic sublattice of Pn.

Table 5. Comparison of the crystal structures of pnictides ATPn (A = Li, Na, K; T = Zn, Cd; Pn = P, As, Sb, Bi)

ATPn		KZnPn	KCdPn	NaZnPn	NaCdPn	LiZnPn		LiCdPn
						Pn = Sb, Bi	Pn = P, As	
$R_{eff}(A^+)/R_{eff}(T^{2+})$ [13, 14]		2.05	1.65	1.54	1.24	1.09		0.88
Structural type [7]		ZrBeSi	PbFCl		MgSrSi	LiGaGe	MgAgAs	
Space group		$P6_3/mmc$	$P4/nmm$		$Pnma$	$P6_3mc$	$F\bar{4}3m$	
Coordination polyhedron (coordination number in parentheless)*	A	TrAP (6)	TP (5)		TP (5)	Tr (3)	T (4)	
	T	Tr (3)	T (4)		T (4)	T (4)	T (4)	
	Pn	TTrP (9)	MTA (9)		MTA (9)	MTrA (7)	C (8)	

* C is cube, MTA is monocapped tetragonal antiprism, MTrA is monocapped triangular antiprism, T is tetrahedron, TP is tetragonal pyramid, Tr is triangle, TrAP is triangular antiprism, TrP is triangular prism, TTrP is three-capped triangular prism.

The consideration performed makes doubtful the assumption [6] about the possibility of the polymorphous transition from the structural type LiGaGe (space group $P6_3mc$) to the structural type MgSrSi (space group *Pnma*), since the characteristic ratios $R_{eff}(A^+)/R_{eff}(T^{2+})$ differ appreciably for these structural types.

Thus, the crystallization from a solution in liquid bismuth gave single crystals of two earlier unknown bismuthides: NaZnBi and NaCdBi. Their crystal structures were determined by single-crystal X-ray structure analysis. In spite of the same stoichiometry and similar coordination polyhedra of Na, Zn/Cd, and Bi atoms, these compounds are of different structural types and form isostructural series with lighter pnictide analogs: NaZnBi and other NaZnPn (Pn = P, As, Sb) crystallize in the structural type PbFCl, whereas NaCdBi (similarly to NaCdPn (Pn = As, Sb)) is of the structural type MgSrSi. The detailed consideration of specific features of the geometry of the coordination polyhedra of the component atoms shows that the ratio of effective ionic radii $R_{eff}(A^+)/R_{eff}(T^{2+})$ is an important factor affecting the occurrence of this or another structural type in compounds ATPn (A is alkaline metal, T is 12 Group (Zn, Cd), and Pn is pnictogen).

It should be mentioned that the synthesized compounds contain bismuth atoms in the formally negative oxidation state and exhibit a fairly high reactivity (especially layered and instable in air NaZnBi), which makes the considered compounds to be promising precursors for the synthesis of bismuth clusters using nonaqueous solvents. For example, the bismuth cluster cations were synthesized [24] by the comproportionation of metallic bismuth and Bi^{3+} in liquid $GaBr_3$, and an idea of the mild reduction of Bi^{3+} in nonaqueous media was successfully accomplished [25].

FUNDING

This work was supported by the RNF-DFG foundation (project no. 19-43-04129) and the Ministry of Science and Higher Education of the Russian Federation in terms of performing the state assignment "Physics of High-Temperature Superconductors and Novel Quantum Materials" (project no. 0023-2019-0005).

CONFLICT OF INTEREST

The authors declare that they have no conflicts of interest.

REFERENCES

1. Ren, Z.-A. and Zhao, Z.-X., *Adv. Mater.*, 2009, vol. 21, no. 45, p. 4584.
2. Bennett, J.W., Garrity, K.F., Rabe, K.M., et al., *Phys. Rev. Lett.*, 2012, vol. 109, no. 16, p. 167602.
3. Yang, J., Wegner, A., Brown, C.M., et al., *Appl. Phys. Lett.*, 2018, vol. 113, no. 12, p. 122105.
4. Schuster, H.-U. and Achenbach, G., *Z. Naturforsch. B: Chem. Sci.,* 1978, vol. 33, p. 113.
5. Zhang, X., Liu, Q., Xu, Q., et al., *J. Am. Chem. Soc.*, 2018, vol. 140, no. 42, p. 13687.
6. Bennett, J.W., Garrity, K.F., Rabe, K.M., and Vanderbilt, D., *Phys. Rev. Lett.*, 2013, vol. 110, no. 1, p. 017603.
7. Ovchinnikov, A. and Bobev, S., *J. Solid State Chem.*, 2019, vol. 270, p. 346.
8. Krenkel, B., Tiburtius, C., and Schuster, H.-U., *Z. Naturforsch. B: Chem. Sci.*, 1979, vol. 34, p. 1686.
9. Savelsberg, G. and Schäfer, H., *Z. Naturforsch., B: Chem. Sci.*, 1978, vol. 33, no. 4, p. 370.
10. Kahlert, H. and Schuster, H.-U., *Z. Naturforsch., B: Chem. Sci.,* 1976, vol. 31, p. 1538.
11. Sheldrick, G.M., *Acta Crystallogr., Sect. C:* Struct. Chem., 2015, vol. 71, no. 1, p. 3.
12. Sheldrick, G.M., *Acta Crystallogr., Sect. A: Found. Adv.*, 2015, vol. 71, no. 1, p. 3.
13. Eisenmann, B. and Somer, M., *Z. Naturforsch., B: Chem. Sci.*, 1985, vol. 40, no. 11, p. 1419.

14. Shannon, R.D. and Prewitt, C.T., *Acta Crystallogr., Sect. B: Struct. Crystallogr. Cryst. Chem.*, 1969, vol. 25, no. 5, p. 925.

15. Shannon, R.D. and Prewitt, C.T., *Acta Crystallogr., Sect. B: Struct. Crystallogr. Cryst. Chem.*, 1970, vol. 26, no. 7, p. 1046.

16. Kushwaha, S.K., Krizan, J.W., Feldman, B.E., et al., *APL Materials*, 2015, vol. 3, no. 4, p. 041504.

17. Xia, S. and Bobev, S., *J. Solid State Chem.*, 2006, vol. 179, no. 11, p. 3371.

18. Reshak, A.H. and Auluck, S., *Comput. Mater. Sci.*, 2015, vol. 96, p. 90.

19. Jaiganesh, G., Merita Anto Britto, T., Eithiraj, R.D., et al., *J. Phys.*, 2008, vol. 20, no. 8, p. 085220.

20. Charifi, Z., Baaziz, H., Noui, S., et al., *Comput. Mater. Sci.*, 2014, vol. 87, p. 187.

21. Schucht, F., Dascoulidou, A., Muller, R., et al., *Z. Anorg. Allg. Chem.*, 1999, vol. 625, p. 31.

22. Schuster, H.-U. and Schroeder, G., *Z. Naturforsch. B: Chem. Sci.,* 1972, vol. 27, p. 81.

23. Winter, F., Pöttgen, R., Greiwe, M., et al., *Rev. Inorg. Chem.*, 2015, vol. 35, no. 1, p. 1.

24. Kuznetsov, A.N., Popovkin, B.A., Henderson, W., et al., *Dalton Trans.*, 2000, no. 11, p. 1777.

25. Kuznetsov, A.N., Popovkin, B.A., Stahl, K., et al., *Eur. J. Inorg. Chem.*, 2005, vol. 2005, no. 24, p. 4907.

Translated by E. Yablonskaya